On the use of the method of moments in plasmonic applications

Guy A. E. Vandenbosch,[1] V. Volski,[1] N. Verellen,[2] and V. V. Moshchalkov[2]

Received 30 November 2010; revised 28 February 2011; accepted 21 March 2011; published 21 May 2011.

[1] In the last 40 years the method of moments (MOM) has been a cornerstone in the field of computational electromagnetics. Traditionally, this method has been used to solve integral equations formulated for antennas and other components in the microwave frequency range and below. In this paper, the application of MOM in the field of plasmonics is briefly reviewed. First, existing literature is referenced. Then the differences with the classical implementations are pointed out. Finally, its applicability, advantages, and disadvantages are discussed. This is done by comparing it with a numerical finite difference time domain solver well-known in the plasmonics research community for a number of example structures. It is shown that also at these higher frequencies, namely in the IR and optical range, MOM is a very powerful technique.

Citation: Vandenbosch, G. A. E., V. Volski, N. Verellen, and V. V. Moshchalkov (2011), On the use of the method of moments in plasmonic applications, *Radio Sci.*, *46*, RS0E02, doi:10.1029/2010RS004582.

1. Introduction

[2] In electromagnetics, numerical techniques have been essential in the development of new technology in the last two decades. The rapidly growing computer capacity and calculation speeds make accurate solutions of very complex problems feasible. This has been especially true in the design of antennas. Whereas 30 years ago, the design of an antenna was based on simple analytical models, or trial and error strategies, nowadays, simulations seem to be as crucial to the design as real measurements. The first practical codes were based on integral equations, solved with the method of moments (MOM) [*Aronson et al.*, 1967]. They offered a very good approximation for the computational capacity available at that time. Later, differential equation techniques like the finite element method (FEM), and the finite difference time domain (FDTD), and other related techniques, also were heavily developed and adopted by the community. A good overview on the comparison of the different computational techniques can be found in the works of *Miller* [1988] and *Peterson et al.* [1998]. The core differences between integral and differential equation techniques are of course well-known: (1) the prenumerical analytical effort required to set up the calculation procedure, (2) the solution domain that has to be discretized, and (3) the implementation of the radiation condition, especially important for antennas. MOM requires a considerably greater analytical effort of the code developer. However, only components sustaining currents need to be discretized. This gives rise to a relatively small number of unknowns. The radiation condition is automatically included. These observations make the MOM an ideal candidate to analyze in a very efficient way a certain category of topologies. Nevertheless, nowadays the emphasis in the user community of computational tools has clearly shifted toward differential techniques. This is due to the combination of two factors: the enormous increase in available computer resources and the generality of these techniques. Since differential techniques in principle are able to analyze virtually anything, the investment in such a tool is very attractive from a budget point of view. As a consequence, many topologies which are inherently more suited for MOM tools, are analyzed and/or designed in literature with slower tools based on differential techniques. This does not mean that MOM tools have disappeared. They are indispensable in problems involving large scatterers, topologies in layer structures with very thick and/or thin layers, configurations with sharp edges, etc. Actually, it is a recent trend of some major differential software tool vendors to also offer MOM capabilities in their software pallet. Also, in newly emerging fields, the MOM still has its important role to play.

[3] This paper considers the application of MOM in plasmonics, i.e., at very high (IR and optical) frequencies. This research field is now high profile in many physics departments all over the world. It can easily be checked that, although there are some papers using the method of moments [*Gallinet and Martin*, 2009; *Kern and Martin*, 2010; *Gallinet et al.*, 2010; *Chremmos*, 2010; *Alegret et al.*, 2008; *Smajic et al.*, 2009], most researchers use differential equation tools to perform their research [see, e.g., *Kappeler et al.*, 2007; *Qiang et al.*, 2004; *Verellen et al.*, 2009]. In most cases the integral equation formulation used is a surface integral equation [*Gallinet and Martin*, 2009; *Kern and Martin*, 2010; *Gallinet et al.*, 2010]. *Chremmos* [2010] uses a magnetic type scalar integral equation to describe surface plasmon scattering by rectangular dielectric channel discontinuities. Even the use of the magnetic current formalism to describe holes, classical at microwave frequencies,

[1]Department of Electrical Engineering, Katholieke Universiteit Leuven, Leuven, Belgium.
[2]Institute for Nanoscale Physics and Chemistry, Katholieke Universiteit Leuven, Leuven, Belgium.

0048-6604/11/2010RS004582

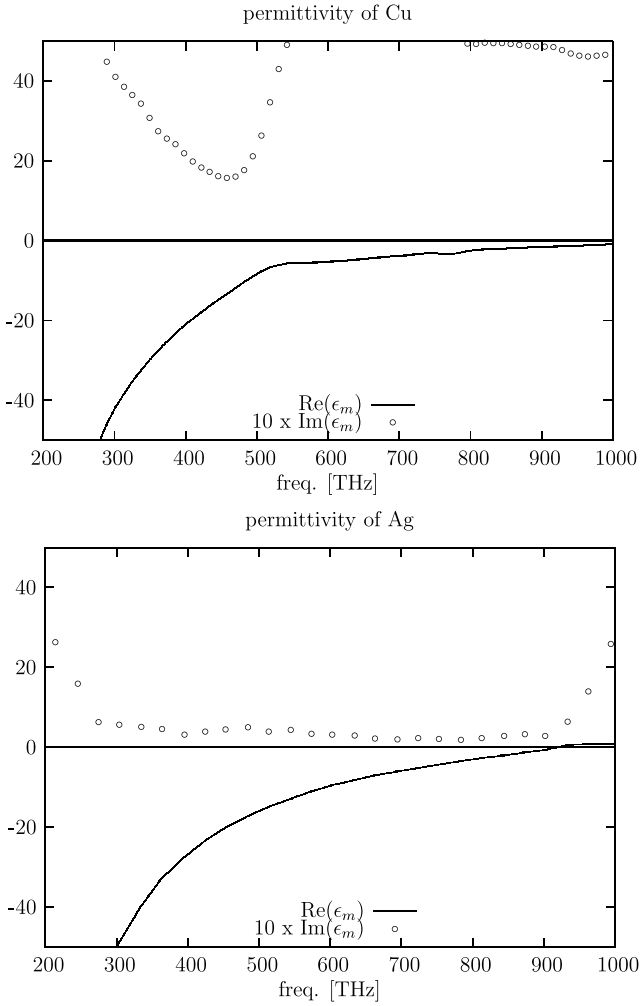

Figure 1. Experimental permittivity of Cu and Ag, both real part and minus the imaginary part (following the conventions in the physics community).

already has been used in plasmonics [*Alegret et al.*, 2008]. In this paper, it will be shown that, in the current status of this research field, MOM should certainly be taken into account as a very competitive computational tool.

2. Microwave and THz Frequencies

[4] This section discusses the differences between a MOM implementation at microwave (and millimeter) wave frequencies, and its extension to IR and optical frequencies. This is done because we observe that there are very few MOM tools in the market that are able to cope with THz frequencies.

2.1. Frequency

[5] The first difference is the frequency itself. Although the order of magnitude is quite different, Mawell's laws are the same. They are linear, and thus scalable. As long as quantum effects do not have to be taken into account, which is still the case for our applications at THz [*Ahmed et al.*, 2010], there is no fundamental problem. The underlying formulation of Maxwell's equations can remain unaffected.

2.2. Three-Dimensional Volumes

[6] A consequence of the high frequencies is the small scale: the elementary building blocks of the topologies considered, e.g., single antenna elements, are at nanoscale. Using the terminology of microwave and millimeter wave computational electromagnetics, at the nanoscale fabrication technology of today is only able to generate 3-D type structures (i.e., volumes). Thin 2-D sheets, where the thickness of the metal is orders of magnitude smaller than the transversal dimensions of the pattern, as commonly used at microwave frequencies (for example a conducting strip or patch), are not possible. This invokes the need for either a real volumetric MOM implementation or the more common surface approach, to handle these 3-D objects. The surface approach has already been used, for example, by *Smajic et al.* [2009]. For realistic structures, the volumetric approach as described by *Schols and Vandenbosch* [2007], where volumes can be embedded within a layer structure, offers clear advantages. All layers form part of the background layered medium, which does not have to be discretized. Note that one of the reasons why at microwave frequencies MOM is being abandoned more and more for FEM and FDTD, i.e., the small transversal size of the layer structures (PCB, laminates, etc.), is not an issue here. At these very high frequencies, in by far most structures the transversal dimensions are electrically huge. Edge effects become almost negligible.

2.3. Material Characteristics

[7] At microwave frequencies, in most cases the material properties are constant over the frequency bands considered. Also, apart from the losses, most metals behave more or less in the same way, i.e., as good conductors. At IR and optical frequencies however, most metals have very dispersive properties. Permittivities and conductivities may vary orders of magnitude over these frequency bands. The real part of the permittivity may even be negative. In Figure 1, the permittivity of Cu and Ag are depicted, both real and imaginary part, which is equivalent to conductivity. These data were obtained through experimental ellipsometry. Note that the difference between the two metals is enormous. It is evident that this strong variation has a serious impact on the behavior of a device over the frequency band. The variability of material characteristics thus has to taken into account into the algorithm. Although this may seem trivial, in some cases, more severe consequences occur. For example, Green's function asymptotes also change over the band considered, and any implementation of MOM assuming a constant asymptotic behavior (for example in an asymptotic extraction technique in order to reduce calculation times) needs this essential relaxation into its formalism. An advantage of a frequency domain technique like MOM compared to a time domain technique like FDTD is that the ellipsometric measurement data can be used directly in the tool, without any further fitting. FDTD techniques developed for the optical range tend to fit the dielectric response of the metal to the experimentally determined dielectric permittivity using a Drude model [*Qiang et al.*, 2004].

3. Comparison of MAGMAS and LUMERICAL

[8] In this section, an in-house developed tool based on the method of moments, called MAGMAS and fully

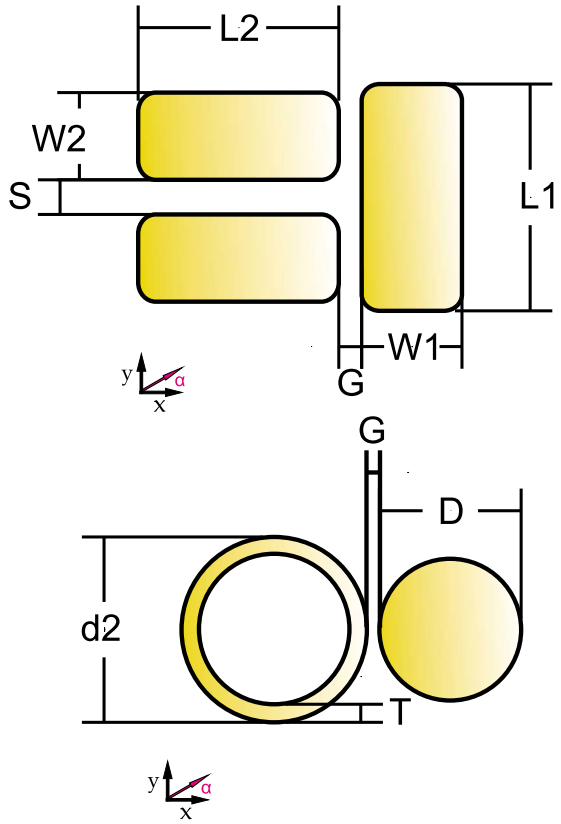

Figure 2. Dolmen and RNDC geometries.

described by *Schols and Vandenbosch* [2007], *Vandenbosch and Van de Capelle* [1992], *Demuynck et al.* [1998], and *Vrancken and Vandenbosch* [2003], is presented and validated for plasmonic applications. MAGMAS was developed for planar and quasi-3-D antenna structures at RF and microwave frequencies. Before MAGMAS could be used for plasmonic applications it had to be considerably upgraded, taking into account the issues raised in the discussion of section 2. The validation is accomplished through a cross comparison with the FDTD solver widely used in this research community Lumerical (http://www.lumerical.com). The analysis shows that MAGMAS can predict also at these frequencies all the relevant parameters of nano structures, just as it did at microwave frequencies for classical antenna problems.

3.1. Structures Under Study

[9] In order to validate the MOM tool and to study the differences with the FDTD tool, three structures are analyzed. The first one is a gold monomer. Its dimensions are 250 nm × 40 nm × 40 nm. The second one, named Dolmen because of the resemblance with the neolithic stone arrangement, was first introduced and theoretically studied by *Zhang et al.* [2006], where Zhang et al. analyzed the plasmon induced transparency in metamaterials made of periodic configurations of this topology. The third one, a Ring Near Disc Cavity (RNDC), was introduced by *Verellen et al.* [2009]. Dolmen and RNDC structures were both analyzed by *Verellen et al.* [2009]. *Verellen et al.* [2009] experimentally demonstrated the effect of symmetry breaking with the observation of predicted Fano resonances in extinction cross sections. The geometries of the second and third structure are depicted in Figure 2. For the Dolmen the thickness of the gold layer is 60 nm. Dimensions in nm are $L_1 = 260$, $L_2 = 230$, $W_1 = 115$, $W_2 = 100$, $S = 50$, $G = 13$. For the RNDC the thickness of the gold layer is 30 nm. The dimensions are $d_2 = 425$, $D = 325$, $T = 80$, $G = 20$, all in nm. As a consequence of the fabrication etching process, the sidewalls of the particles are slanted with an angle of approximately 20 degrees [*Verellen et al.*, 2009]. SEM (scanning electron microscope) images of both structures can be seen in Figures 5c and 6c. All structures are placed onto a crystal substrate modeled with $n = 1.5$ constant refractive index.

3.2. Modeling Details

[10] In order to study the convergence of both MOM and FDTD, structure 1 was analyzed with different mesh densities (see section 3.3). For structures 2 and 3, the mesh in Lumerical was defined by 2.5 nm side cubes in a 2.5 × 2.5 × 0.75 microns box. In MAGMAS, a hexahedron mesh was used for the metallic components. The Dolmen thickness was meshed with 5 subdivisions. The mesh in the monomer and the dimer was based on 19.16 × 20 × 12 and 20.9 × 20 × 12 (units in nm) hexahedral unit cells, respectively, yielding a total of 3263 rooftop basis functions. For the RNDC a staircase approximation was needed to describe both ring and disc elements. To that purpose a finer mesh was required in the horizontal plane, therefore limiting the number of subdivisions in z direction. The resulting mesh consists of 25 × 25 × 10 and 13.3 × 13.28 × 10 (units in nm) hexahedral unit cells for disc and ring, respectively. Note that the mesh in the case of the ring is much finer, to accurately approximate its constant width (Figure 3). This configuration yields a total of 6390 rooftop basis functions. It is important to mention that the effect of the slanted edges was not modeled in MAGMAS, although it was considered in Lumerical. The reason is the fact that a quasi-3-D formulation is used for the integral equations that are solved within MAGMAS (for more details, see *Schols and Vandenbosch* [2007]). The substrate was modeled with a semi-infinite half-space. Of course, it was actually cut by the finite simulation box in Lumerical. In both softwares the structures were illuminated with a plane wave, coming from the top side in the case of Lumerical, and from the bottom side in the case of MAGMAS. This difference does not affect the cross sections obtained. Extinction cross sections were calculated in MAGMAS from the far field by applying the Optical Theorem [*Newton*, 1976], and in Lumerical as the sum of scattering and absorption cross sections.

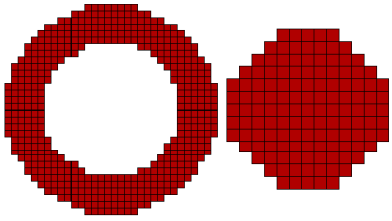

Figure 3. RNDC MAGMAS mesh top view.

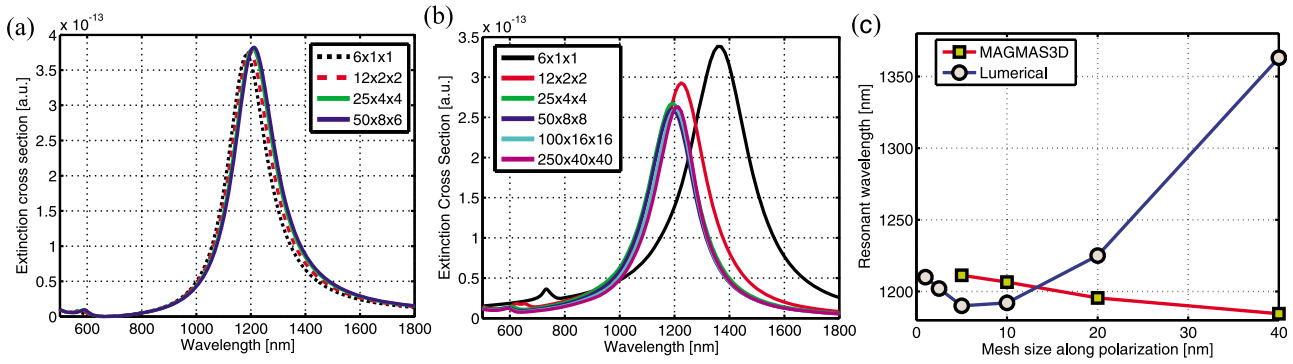

Figure 4. (a and b) Extinction cross section of a 250 nm × 40 nm × 40 nm gold monomer on a substrate with n = 1.5 (MAGMAS 3-D (Figure 4a) and Lumerical (Figure 4b)). (c) Convergence performance of both solvers.

3.3. Numerical Results

[11] Figure 4 shows the extinction cross section obtained for the first structure, the gold monomer. The data clearly demonstrate the by far superior stability of MOM for this type of structure. The results obtained even with a very rough mesh (6 × 1 × 1, 41.7 nm × 40 nm × 40 nm) provide already a very good estimate of the resonance. The differences in extinction cross section calculated with the rough and fine meshes are almost negligibly small. Extinction cross sections calculated with FDTD, as expected, depend considerably on the chosen mesh. A fine mesh should be used for reliable calculations. Note that in contrast to MOM, for FDTD also the levels clearly depend on the mesh. The calculated wavelengths as a function of the mesh cell size are plotted in Figure 4c.

[12] Information on the calculation times is given in Table 1. It has to be emphasized that calculation times cannot be directly compared. The computers used were different, and the FDTD tool used 10 processors in parallel. Further, since it is a time domain technique, a calculation time per frequency point cannot be given for FDTD. Nevertheless, combining the data in Table 1 with the data concerning the convergence, given in Figure 4, it is easily seen that MOM outperforms FDTD.

[13] Figure 5 shows the extinction cross sections obtained for structure two, i.e., for monomer, dimer, and Dolmen, respectively, with the two tools. Values have been normalized with respect to the maximum peak. The similarity is evident in all cases, even with the rougher mesh used in MAGMAS. For the monomer polarized along its axis, there is only a redshift of 50 nm with respect to Lumerical. The peak width is slightly broader in MAGMAS. Both facts can be explained by the slanted edges, not taken into account in this solver, and by the different mesh employed. Notice a second peak of much smaller amplitude appearing around 550 nm, found by both solvers.

[14] Figure 5b shows the results for the dimer with x and y polarizations. The longitudinal polarization cross section exhibits a similar behavior as in the monomer case. There is a small shift of 50 nm and the MAGMAS peak is slightly broader. For the y polarization there is a bigger difference. Lumerical presents a narrower peak at 620 nm accompanied by a small dip at 600 nm and another smaller peak at 580 nm. In MAGMAS however a single smooth peak is found. This can be explained by the rough mesh and the not taking into account of the slanted edges.

[15] Figure 5c depicts the case of the full Dolmen structure. The polarization along the x axis reveals a similar behavior of the extinction as for the dimer, but shifted and broadened. MAGMAS is again about 50 nm redshifted and broader. The two small peaks appearing bellow 700 nm are not so well defined if compared with Lumerical, but are still present with lower amplitude. For the y polarization the shift is not uniform. For the first peak (around 1300 nm) a 60 nm redshift is found whereas for the second one (at 960 nm) there is a 20 nm blueshift. The Fano resonances at 810–820 nm and 1100–1150 nm are qualitatively similar for both solvers. Again, at wavelengths bellow 700 nm three small peaks are seen with Lumerical, and a smoother behavior with MAGMAS.

[16] Figure 6 shows extinction cross sections of disc, ring and RNDC structures. In the case of the disc a similar behavior with MAGMAS and Lumerical is obtained. The first presents a redshift of about 100 nm, bigger than the ones for the Dolmen structure. This can be attributed to the rougher mesh used to model the disc in MAGMAS (Figure 3), which introduces geometric imperfections. There

Table 1. Calculation Times as a Function of the Mesh for the Gold Monomer[a]

MOM		FDTD	
Mesh	Calculation Time per Frequency Point (s)	Mesh	Total Calculation Time (s) (10 Processors in Parallel)
6 × 6 × 1	5.4	6 × 1 × 1	38
12 × 2 × 2	10.4	12 × 2 × 2	55
25 × 4 × 4	33.6	25 × 4 × 4	225
50 × 8 × 6	238	50 × 8 × 8	672
		100 × 16 × 16	5,893
		250 × 40 × 40	20,100

[a]MOM: Intel(R) Xeon(R) CPU E5335 at 2 GHz, 32 Gb memory. FDTD: d1585g6 4× hc CPU at 2.8 GHz, 128 Gb memory.

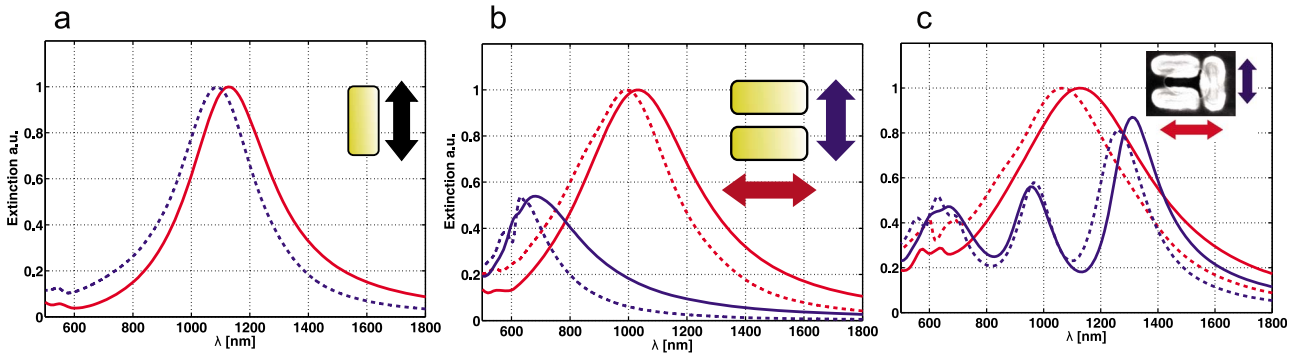

Figure 5. Extinction cross sections for (a) monomer, (b) dimer, and (c) Dolmen. MAGMAS, solid lines; Lumerical, dotted lines.

is also a very small peak around 500 nm with MAGMAS that is not detected with Lumerical. Peak widths are almost identical in both solvers, as well as the slope of the curves at both sides of the maximum. Figure 6b shows the case of the ring. The results are almost identical, and even the so far noticed redshift is not present any more. MAGMAS accurately describes both peaks.

[17] RNDC cross sections for x and y polarizations are depicted in Figure 6c. An offset of 0.4 was applied to the second one to better distinguish both polarizations. A more noticeable difference is observed. For the x polarization extinctions are almost identical above 1500 nm. For smaller wavelengths however, MAGMAS is blue shifted. What is more important, MAGMAS seems more explicit in describing the Fano resonance appearing near 850 nm. The dip at this wavelength is also sensed in Lumerical simulations, but more softened. The shape of the curve obtained with the latter is indeed better fitted to the extinction measured by *Verellen et al.* [2009] for the same structure. The fact that MAGMAS accurately describes these "particular" resonances with even relative rough meshes might be due to their strong dependence on the interparticle distance [*Verellen et al.*, 2009]. This distance is spatially sampled in FDTD techniques, whereas MAGMAS calculates the coupling between individual hexahedrons with analytical Green's functions that take into account the exact relative distance. In the case of y polarization there is no symmetry breaking and hence no Fano resonances are observed. Obtained extinctions are quite similar above 1500 nm and bellow 800 nm, but the band in the middle presents some differences. The MAGMAS peak in that band is about 100 nm blueshifted with respect to Lumerical. Also their shape is quite different. The first solver yields an asymmetrical peak that resembles a shark fin, whereas the second yields a peak that is almost symmetrical.

3.4. Comparison With Measurements

[18] In order to assess the accuracy of the simulations in comparison with measurements, two structures were fabricated and measured: the monomer and the disc. The confocal acquisition of the spectra is described in detail by *Verellen et al.* [2009]. Briefly, the radiation of a white light supercontinuum is polarized and then focused on the sample with a 10 × microscope objective. The light transmitted through the sample is collected by a 50 × IR corrected microscope objective and spatially filtered by the entrance of an optical fiber in order to select only the signal coming from the focal region. The signal is then guided via the fiber to the detectors, a silicon CCD and APD for energies higher than 1.6 eV, and InGaAs below.

[19] The results are given in Figure 7. The values are not normalized with respect to the maximum. In general, the agreement between simulations and measurements is obvious. Simulations clearly can be used to predict resonances in

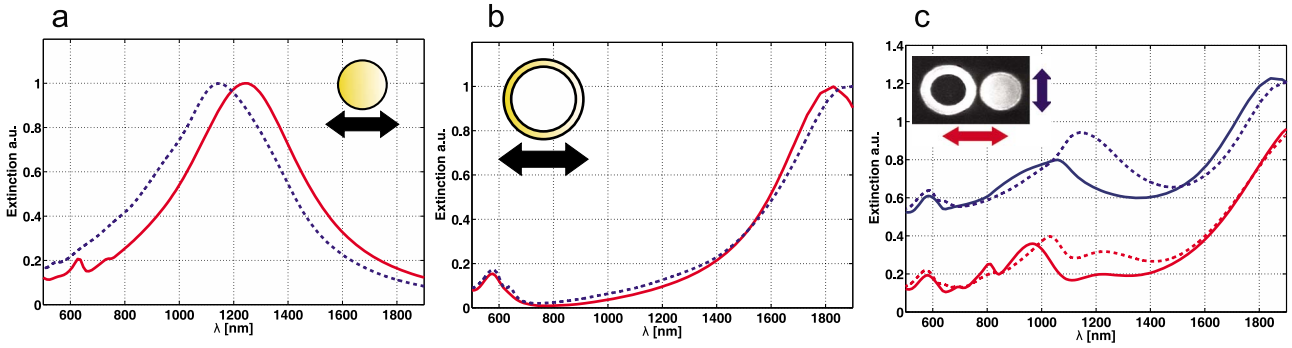

Figure 6. Extinction cross sections for (a) disc, (b) ring, and (c) RNDC. MAGMAS, solid lines; Lumerical, dashed lines.

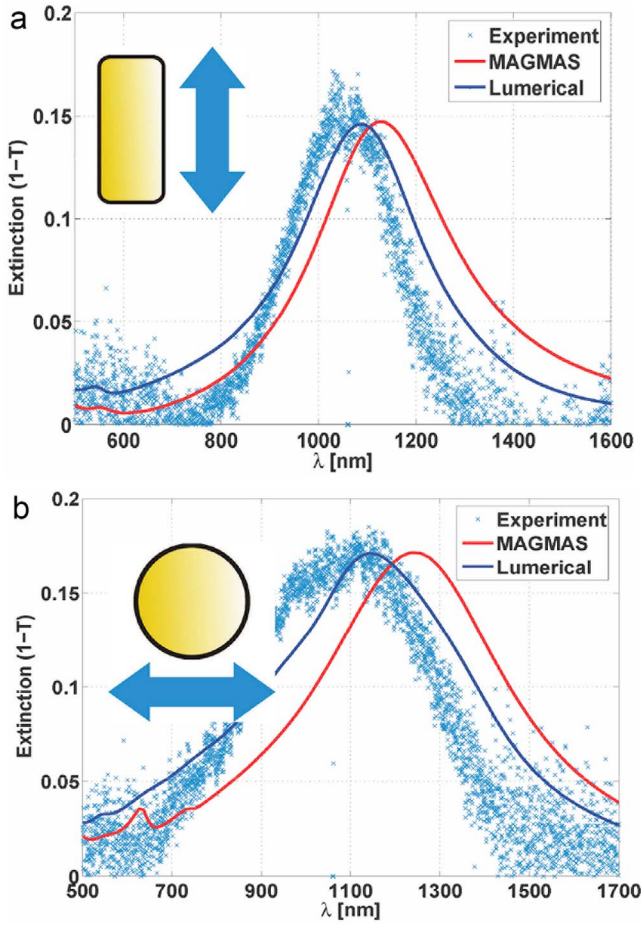

Figure 7. Simulated and measured extinction cross sections for (a) monomer and (b) disc.

extinction cross section. However, the quite high noise level prohibits a comparison of the lower parts. Also, from the measurements it is impossible to decide which one of the simulations is the most accurate.

4. Conclusion

[20] The technique of describing component topologies by solving integral equations with the MOM is not widespread in plasmonics. Also, this field of research is still not "conquered" by the commercial MoM software vendors, unlike for example the field of designing antennas or microwave circuits. As a consequence, to the best knowledge of the authors, at this moment all literature on this topic uses in-house built solvers. However, in this paper it is proven that the MOM technique does have a real potential in this research community. It keeps all the advantages that it had since the beginning at RF and microwaves: robustness, fast convergence, and an intrinsically lower number of unknowns, leading to considerably lower calculation times.

[21] **Acknowledgments.** The authors would like to thank the Fund for Scientific Research Flanders (FWO-V) and the Methusalem program of the Flemish government for their financial support.

References

Ahmed, I., E. H. Khoo, E. Li, and R. Mittra (2010), A hybrid approach for solving coupled Maxwell and Schrödinger equations arising in the simulation of nano-devices, *IEEE Antennas Wirel. Propag. Lett.*, *9*, 914–917.

Alegret, J., P. Johansson, and M. Kall (2008), Green's tensor calculations of plasmon resonances of single holes and hole pairs in thin gold films, *N. J. Phys.*, *10*(10), 105004.

Aronson, E., C. Taylor, and R. Harrington (1967), Matrix methods for solving antenna problems, *IEEE Trans. Antennas Propag.*, *15*(5), 696–697.

Chremmos, I. (2010), Magnetic field integral equation analysis of surface plasmon scattering by rectangular dielectric channel discontinuities, *J. Opt. Soc. Am. A Opt. Image Sci. Vis.*, *27*(1), 85–94.

Demuynck, F. J., G. A. E. Vandenbosch, and A. R. Van de Capelle (1998), The expansion wave concept, part I: Efficient calculation of spatial Green's functions in a stratified dielectric medium, *IEEE Trans. Antennas Propag.*, *46*, 397–406.

Gallinet, B., and O. J. Martin (2009), Scattering on plasmonic nanostructures arrays modeled with a surface integral formulation, *Photonics Nanostructures Fundam. Appl.*, *8*(4), 278–284.

Gallinet, B., A. M. Kern, and O. J. F. Martin (2010), Accurate and versatile modeling of electromagnetic scattering on periodic nanostructures with a surface integral approach, *J. Opt. Soc. Am. A Opt. Image Sci. Vis.*, *27*(10), 2261–2271.

Kappeler, R., D. Erni, X.-D. Cui, and L. Novotny (2007), Field computations of optical antennas, *J. Comput. Theor. Nanosci.*, *4*(3), 686–691.

Kern, A. M., and O. J. F. Martin (2010), Surface integral formulation for 3D simulations of plasmonic and high permittivity nanostructures, *J. Opt. Soc. Am. A Opt. Image Sci. Vis.*, *26*(4), 85–94.

Miller, E. K. (1988), A selective survey of computational electromagnetics, *IEEE Trans. Antennas Propag.*, *36*(9), 1281–1305.

Newton, R. G. (1976), Optical Theorem and beyond, *Am. J. Phys.*, *44*(7), 639–642.

Peterson, A. F., S. L. Ray, and R. Mittra (1998), *Computational Methods for Electromagnetics*, IEEE Press, Piscataway, N. J.

Qiang, R., R. L. Chen, and J. Chen (2004), Modeling electrical properties of gold films at infrared frequency using FDTD method, *Int. J. Infrared Millimeter Waves*, *25*(8), 1263–1270.

Schols, Y., and G. A. E. Vandenbosch (2007), Separation of horizontal and vertical dependencies in a surface/volume integral equation approach to model quasi 3-D structures in multilayered media, *IEEE Trans. Antennas Propag.*, *55*(4), 1086–1094.

Smajic, J., C. Hafner, L. Raguin, K. Tavzarashvili, and M. Mishrickey (2009), Comparison of numerical methods for the analysis of plasmonic structures, *J. Comput. Theor. Nanosci.*, *6*(3), 763–774.

Vandenbosch, G. A. E., and A. R. Van de Capelle (1992), Mixed-potential integral expression formulation of the electric field in a stratified dielectric medium—Application to the case of a probe current source, *IEEE Trans. Antennas Propag.*, *40*, 806–817.

Verellen, N., Y. Sonnefraud, H. Sobhani, F. Hao, V. V. Moshchalkov, P. V. Dorpe, P. Nordlander, and S. A. Maier (2009), Fano resonances in individual coherent plasmonic nanocavities, *Nano Lett.*, *9*(4), 1663–1667.

Vrancken, M., and G. A. E. Vandenbosch (2003), Hybrid dyadic-mixed-potential and combined spectral-space domain integral equation analysis of quasi-3-D structures in stratified media, *IEEE Trans. Microwave Theory Tech.*, *51*(1), 216–225.

Zhang, S., D. A. Genov, Y. Wang, M. Liu, and X. Zhang (2006), Plasmon-induced transparency in metamaterials, *Phys. Rev. Lett.*, *8*(4), S239–S249.

V. V. Moshchalkov and N. Verellen, Institute for Nanoscale Physics and Chemistry, Katholieke Universiteit Leuven, Celestijnenlaan 200D, B-3001 Leuven, Belgium.

G. A. E. Vandenbosch and V. Volski, Department of Electrical Engineering, Katholieke Universiteit Leuven, Kasteelpark Arenberg 10, B-3001 Leuven, Belgium. (guy.vandenbosch@esat.kuleuven.be)